THE JOURNAL OF PHYSICAL CHEMISTRY C

Article

pubs.acs.org/JPCC

Molecular Design Principles for Magneto-Electric Materials: All-Electric Susceptibilities Relevant to Optimal Molecular Chromophores

Alexander J.-T. Lou,[‡,†] Elizabeth F. C. Dreyer,[‡,§] Stephen C. Rand,[*,§] and Tobin J. Marks[*,†]

[†]Department of Chemistry and the Materials Research Center, Northwestern University, Evanston, Illinois 60208, United States

[§]Center for Dynamic Magneto-Optics, Department of Electrical Engineering & Computer Science, University of Michigan, Ann Arbor, Michigan 48109-2099, United States

Supporting Information

ABSTRACT: Magneto-electric (M-E) response at the molecular level arises from the interaction of matter with the electric and magnetic fields of light, and can manifest itself as nonlinear M-E magnetization (M_{NL}) or M-E rectification (P_{NL}). However, there is presently a limited understanding of how molecular material properties impact M-E response. Here we investigate the relationship between M-E nonlinear coefficients and the third-order electric susceptibility, $\chi^{(3)}$, finding that M_{NL} is proportional to $\chi^{(3)}_{xxxx}$ while P_{NL} scales with $\chi^{(3)}_{zzxx}$ due to a cascaded nonlinearity. By applying a sum-over-states (SOS) expression for the elements of $\chi^{(3)}$ to valence-bond charge-transfer (VB-CT) models, we formulate practical guidelines for the design of materials expected to exhibit enhanced M-E properties. On this basis, we predict that many conventional nonlinear optical chromophores with large values of $\chi^{(3)}_{xxxx}$ may be suitable for generating optical magnetism at low intensities. In the case of M-E rectification, analysis of Λ-shaped, X-shaped, and octupolar VB-CT models suggests that their molecular structures can be tuned to enhance the response by maximizing $\chi^{(3)}_{zzxx}$. In particular, octupolar molecules with a predominantly CT character ground state and Λ-shaped chromophores with weakly conjugated bridges between donor and acceptor moieties should promote off-diagonal nonlinearity and M-E rectification.

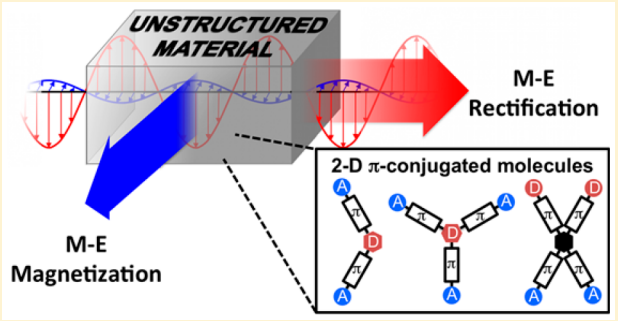

1. INTRODUCTION

A multitude of useful phenomena arise from the interaction of matter with intense light fields. Those resulting from the electric field component of the light are the subject of conventional nonlinear optics (NLO), have been studied for several decades, and find application in a myriad of photonics technologies.[1−9] However, dynamic magnetic interactions are also possible, and can give rise to unique properties such as negative permeability,[10] negative refraction,[11] and the prospects of completely new phenomena or capabilities, including cloaking and super lensing.[12−16] Thus far, magnetic interactions have only been demonstrated in specialized photonic nanostructures and ultrahigh energy systems.[17] In unstructured materials, it has long been presumed that the strength of magnetic interactions is unavoidably weak, so that the possibility of nonlinear magneto-electric interactions has gone unexplored. It was only recently that the dynamic magneto-electric (M-E) effects previously neglected in the common description of polarization were shown to be surprisingly strong in dielectric liquids and crystalline solids.[18,19]

Dynamic M-E effects (Figure 1) can manifest as magnetization $M_y(\omega)$ or rectification $P_z(0)$, both of which have exciting potential applications. Of particular interest here is the possibility of converting light to electricity via M-E rectification, in a capacitive manner that avoids the fundamental limitations of conventional photovoltaic (PV) technologies and substantially circumvents the cogeneration of heat.[20] Furthermore, optical magnetization may enable the generation of internal magnetic fields useful for extending the distance over which carrier spin orientation is preserved in spintronic circuitry, or enable ultrafast reading and writing of magnetic memories, or induce negative permeability in natural dielectric materials.[21] The generation of strong, high frequency magnetic fields has been challenging historically,[10] so any advances in magnetism at optical frequencies are likely to afford unforeseen applications.

Polarization contributions from the M-E susceptibility (χ_{ME}) can be described classically by considering the combined forces of electric and magnetic fields, $E_x(\omega)$ and $H_y(\omega)$, exerted on a bound electron by light propagating along the z-axis (Figure 1). The induced motion can be understood as follows: (1) $E_x(\omega)$ initiates electronic motion and displacement parallel to the electric field; (2) the orthogonal $H_y(\omega)$ field imparts a Lorentz

Received: May 5, 2017
Revised: June 29, 2017
Published: July 3, 2017

DOI: 10.1021/acs.jpcc.7b04307
J. Phys. Chem. C 2017, 121, 16491−16500

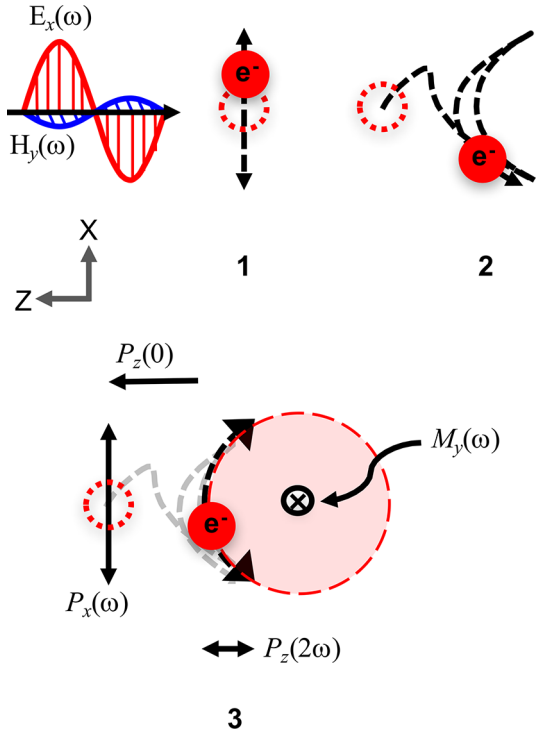

Figure 1. Classical depiction of M-E polarization with light propagating from right to left: (1) *E*-field only initiates motion in the *x* direction, (2) Lorentz force and parametric enhancement causes displacement along *z*, and (3) final arc-like trajectory produces magnetization in the *y* direction. Dashed lines depict electron motion and displacement; the labeled arrows are components of polarization and magnetization. The dotted red outlined circle indicates the starting position of the bound electron.

force that deflects the motion in the direction of propagation (*z*-axis); (3) As a result, an electron initially at rest is induced to follow an arc-like trajectory in the *xz* plane, producing three M-E nonlinearities: magnetization $M_y(\omega)$, rectification $P_z(0)$, and second harmonic generation $P_z(2\omega)$. These three magneto-electric moments thus arise from a 2-step (2-photon) high-field process in which the electric field interaction takes place first, and the magnetic field interaction is second, making them proportional to the electric dipole transition moment.[21] The discovery of these M-E effects calls for a more complete description of nonlinear response that includes second- and third-order M-E contributions ($\chi^{(2)}_{ME}$ and $\chi^{(3)}_{ME}$), as well as conventional first ($\chi^{(1)}$), second ($\chi^{(2)}$), and third-order ($\chi^{(3)}$) all-electric terms in eqs 1 and 2.

$$P_{NL} = \varepsilon_0\{\chi^{(1)}E(\omega) + \chi^{(2)}E(\omega)E(\omega) + \chi^{(3)}E(\omega)E(\omega) E(\omega) + ...\} + (1/c)\{\chi^{(2)}_{ME}H(\omega)E(\omega) + \chi^{(3)}_{ME}E(\omega)H(\omega) E(\omega) + ...\} \quad (1)$$

$$M_{NL} = \{\chi^{(2)}_{ME}E(\omega)H(\omega) + \chi^{(3)}_{ME}E(\omega)H(\omega)E(\omega) + ...\} \quad (2)$$

The details of the quantum theoretical and classical description, as well as numerical simulations of M-E nonlinearity in model systems have been reported in the literature,[19,22,23] and M-E magnetization has been observed experimentally as magnetic dipole (MD) scattering in dielectric liquids, crystals, and glasses.[24] Recent investigations[23,24] have shown that the strength of induced magnetic scattering depends on the details of the molecular structure, notably the moment of inertia in the case of small molecules in liquids. However, to date, few tools have been available to understand structure−property relationships in M-E materials at the molecular level, and to direct the development of materials with enhanced M-E coefficients for rectification and magnetization. In this contribution, we derive and exploit new relationships between the M-E coefficients for rectification and magnetization and elements of the third-order susceptibility $\chi^{(3)}$ in order to develop useful design criteria. For example, the static polarization created within centrosymmetric materials by M-E rectification is shown to mediate a cascaded nonlinearity combining rectification and an induced electro-optic response that yields nonlinear refraction (see Supporting Information). An equivalence is established between the M-E coefficient for rectification and the off-diagonal element $\chi^{(3)}_{zzxx}$ of the third-order susceptibility tensor. A similar equivalence is found between the M-E coefficient for magnetization and the diagonal element $\chi^{(3)}_{zzxx}$. These results permit us to employ empirical information and theoretical analysis of structure−function relationships in $\chi^{(3)}$ materials to predict the performance of magneto-electric materials at the molecular level.

In contrast to the scarcity of studies of M-E material response at the molecular level, the design of materials with large $\chi^{(3)}$ values has been an area of intense interest for several decades, and is now a relatively mature field in terms of understanding structure−property relationships.[25] Therefore, establishing a link between magneto-electric and well-studied third-order susceptibilities is highly desirable. To make an explicit connection with chemical models, we begin by recognizing that the macroscopic NLO susceptibility $\chi^{(3)}$ of bulk materials reflects the microscopic second hyperpolarizability γ of their molecular constituents.

$$\chi^{(3)}(-\omega;\ \omega,\ -\omega,\ \omega) = NL^4(\omega)\gamma(-\omega;\ \omega,\ -\omega,\ \omega) \quad (3)$$

In eq 3,[26] N is the number density of chromophores and $L^4(\omega)$ is the Lorentz local-field factor for a third-order process. In the past, design of high performance NLO chromophores (Figure 2) relied on qualitative but pragmatic structure−property relationships, such as the chemically intuitive sum-over-states (SOS) expression.[27−30] The commonly used three-state version of the SOS expression for the diagonal element γ_{xxxx} of the second hyperpolarizability is given by eq 4.[31−33]

$$\gamma_{xxxx} \propto -\frac{(\mu_{01}{}^x)^4}{E_{01}{}^3} + \frac{(\mu_{01}{}^x\Delta\mu_{01}{}^x)^2}{E_{01}{}^3} + \frac{(\mu_{01}{}^x\mu_{12}{}^x)^2}{E_{01}{}^2E_{02}} \quad (4)$$

Here, μ_{ij} is the transition dipole moment between states *i* and *j*, $\Delta\mu_{ij}$ is the difference between the state dipole moments μ_i and μ_j, and E_{ij} is the transition energy. Several well-known approaches to increase γ_{xxxx} stem from this model, such as bond length alternation (BLA), judicious choice of donor and acceptor moieties, disrupted conjugation, or a combination of these approaches.[27,29,30,34−37]

In this work, we focus on heuristic valence-bond charge-transfer (VB-CT) models to provide a broadly applicable approach to enhancing specific elements of $\chi^{(3)}$. VB-CT models[38−43] provide a physical description of molecular electronic structure based on the relative contributions of VB and CT resonances to the ground state, and are particularly well-suited to capture the most salient features of molecular NLO response. Previously, the SOS based analysis of dipolar, Λ-shaped, octupolar, and tetrahedral push−pull VB-CT models afforded an improved understanding of lower order polarization in such molecules. The same models can be used to understand

DOI: 10.1021/acs.jpcc.7b04307
J. Phys. Chem. C 2017, 121, 16491−16500

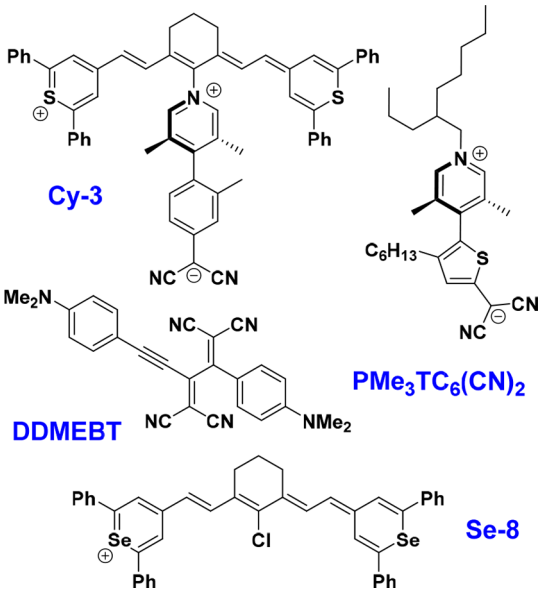

Figure 2. Known high-performance third-order NLO chromophores. Hybrid cyanine-twisted π-system (TICT) chromophore, **Cy-3**; TICT chromophore, $\mathbf{PMe_3TC_6(CN)_2}$; cross-conjugated chromophore, **DDMEBT**; high performance cyanine chromophore, **Se-8**, are representative materials that emerged by applying a "designer" approach to enhancing NLO response.

third-order polarization.[40−43] In order to create design rules for enhanced M-E rectification or magnetization, we therefore draw on the predictions of a simplified SOS expression applied to VB-CT models for the second hyperpolarizability, γ, after establishing a link between the M-E susceptibilities of main interest here, $\chi^{(2)}_{ME} \equiv \chi^{(eme)}$ and $\chi^{(3)}_{ME} \equiv \chi^{(meme)}$, and elements of the all-electric third-order susceptibility $\chi^{(3)}$.

2. THEORETICAL LINKS BETWEEN SECOND-ORDER AND THIRD-ORDER NONLINEAR OPTICAL SUSCEPTIBILITIES

In this section, we establish an explicit connection between magneto-electric coefficients for P_{NL}, M_{NL} and individual elements of the all-electric susceptibility $\chi^{(3)}$. The constitutive relations for the two magneto-electric (M-E) processes of interest are first expressed in terms of equivalent electric fields. They are then compared with expressions for all-electric four-wave mixing polarizations driven by the same input fields. Finally, correspondences are identified between the various coefficients. In this section, we summarize the results for both M-E rectification and magnetization that are analyzed in complete detail in the Supporting Information (SI).

Unlike the polarizations of conventional nonlinear optics that only take electric field components into account, the moments described by constitutive relations of M-E processes contain magnetic fields. For these processes to be compared with all-electric nonlinearities, their fields must be converted to equivalent electric fields in accordance with Maxwell's equations. For x-polarized light propagating along the z-axis the transverse components are found from Faraday's law to be related by

$$H_y^* = -E_x^*/\eta_0 \tag{5}$$

where η_0 is the electromagnetic impedance. This relation is therefore used throughout the present work to convert the moments encountered in M-E rectification and M-E magnetization to equivalent, all-electric expressions.

We begin by clarifying notation and the order of the two main susceptibilities on which this analysis focuses. The susceptibility governing ME rectification mediates a second-order polarization

$$P_{NL} = (1/c)\chi^{(eme)}H^*E \tag{6}$$

as given in eq 1. The coefficient $\chi^{(eme)}$ has superscripts that specify the electric (e) or magnetic (m) character of the fields involved in the nonlinearity, ordered from right to left in sequence. Thus, *eme* specifies an electric field followed by a magnetic field, ultimately producing an electric polarization. The second-order induced magnetization M_{NL} has a similar form eq 7.

$$M_{NL} = \chi^{(mme)}H^*E \tag{7}$$

However, the tensor element $\chi^{(mme)}$ for radiative magnetization vanishes in centrosymmetric media when conventional symmetry analysis is applied and is small even when dynamic symmetry-breaking[22] is taken into account (see Supporting Information). Classically, the largest nonvanishing contribution to transverse (radiative) magnetization at the optical frequency is therefore of higher order, namely

$$M_{NL} = \chi^{(meme)}EH^*E \tag{8}$$

In eqs 6 and 8, magneto-electric responses, P_{NL} and M_{NL}, are driven jointly by the electric field E and the magnetic field H of light,[22,44,45] but their frequencies differ since the former is second-order while the latter is third-order. P_{NL} is obtained by combining field components E and H^* at frequencies ω and $-\omega$ respectively to form a static field. M on the other hand oscillates at the optical frequency ω, since it results from the combination of three optical frequencies ($\omega = \omega - \omega + \omega$).

Introducing equivalent fields as prescribed by eq 5, the amplitude of M-E rectification becomes

$$P_z^{(2)} = -\varepsilon_0\chi_{zyx}^{(eme)}E_x^*E_x \tag{9}$$

The indices on the susceptibility tensor refer to the original orientation of the fields, not the equivalent fields, because this element is determined by the actual input field directions rather than their equivalents. Also, there is no Einstein convention regarding repeated indices once index assignments have been made. Cascaded M-E rectification with induced electro-optic response (see the Supporting Information) results in the third-order polarization

$$P_z^{(3)}(\omega) = \varepsilon_0\left\{\frac{[\chi_{zyx}^{(eme)}(0; -\omega, \omega)]^2}{\varepsilon_r(0) - 1}\right\}E_z(\omega)E_x^*(-\omega)E_x(\omega) \tag{10}$$

For third-order M-E magnetization, eq 8 immediately leads to the equivalent expression

$$M_y^{(3)} = -(\chi_{yxyx}^{(meme)}/\eta_0)E_xE_x^*E_x \tag{11}$$

To make a comparison between magneto-electric rectification or magnetization and all-electric nonlinear polarizations, it is just as important to convert the left-hand sides of the constitutive relations to polar vector fields as the right sides. While this is already the case in eq 10, it is not true in eq 11, where the left-hand side is an axial vector. Hence the magnetization must also be converted to an equivalent electric field consistent with Maxwell's equations. An argument based on Ampere's law is used

DOI: 10.1021/acs.jpcc.7b04307
J. Phys. Chem. C 2017, 121, 16491−16500

in the Supporting Information to show that $M_y = -cP_x$ (see eqs S20−S23). Substitution of this into eq 11 yields a satisfactory all-electric equivalent expression for third-order magnetization, which is

$$P_x^{(3)}(\omega) = \varepsilon_0 \chi_{yxyx}^{(meme)} E_x(\omega) E_x^*(-\omega) E_x(\omega) \tag{12}$$

Finally, by comparing the polarizabilities in eqs 10 and 12 with four-wave mixing expressions with the same input driving fields, the key results of this paper may be obtained. Magneto-electric coefficients $\chi_{zyx}^{(eme)}$ and $\chi_{yzyx}^{(meme)}$ are found to obey the following equivalence relations with respect to third-order, all-electric susceptibility elements.

$$\left\{ \frac{[\chi_{zyx}^{(eme)}(0; -\omega, \omega)]^2}{\varepsilon_r(0) - 1} \right\} = \chi_{zzxx}^{(3)} \tag{13}$$

$$\chi_{yxyx}^{(meme)} = \chi_{xxxx}^{(eeee)} \tag{14}$$

The expressions in eqs 13 and 14 establish specific relationships between M-E susceptibilities and third-order susceptibilities which are nonzero in all crystal classes. Because of the extensive prior work on measurement and prediction of third-order susceptibility elements, including analysis of the relationship between structure and function at the molecular level, these connections allow us to formulate guidelines for detailed design of magneto-electric materials at the molecular level. The equivalence relations also imply that magneto-electric rectification and magnetization are universally allowed in dielectric materials of arbitrary crystal symmetry.

3. DESIGNING MOLECULAR MATERIALS TO ENHANCE MAGNETIZATION, M_{NL}

Given eq 14, we may develop design criteria for enhanced M-E magnetization based on the objective of maximizing the diagonal third-order tensor component $\chi_{xxxx}^{(3)}$ (or the second hyperpolarizability element γ_{xxxx}). Serendipitously, γ_{xxxx} governs the response of the vast majority of third-order NLO chromophores, which are essentially one-dimensional in nature (Figure 2), and derive their nonlinearities from low-energy excitations within a π-conjugated backbone.[46,47] A great deal of experimental effort has been directed to optimizing γ_{xxxx} over the past few decades, so we may immediately conclude that *based on the equivalence* relations *developed in* Section 2, *those molecules which exhibit large diagonal third-order nonlinearities are likely to have a large M−E magnetization coefficient.*

4. DESIGNING MOLECULAR MATERIALS TO ENHANCE POLARIZATION, P_{NL}

The relationship between M-E rectification and off-diagonal third-order tensor components $\chi_{zzxx}^{(3)}$ (or γ_{zzxx}), shown in eq 13, is more challenging to exploit for material design. Historically, far less attention has been paid to the off-diagonal elements of γ, as they have no special significance in conventional NLO. To identify promising classes of molecules, we first draw upon literature concerning the lower order polarization, β. Although it is well-known that the specific requirements for enhanced γ_{xxxx} and β_{xxx} are different, the general prerequisites for large β_{xxz} and β_{zxx} are similar to those for γ_{zzxx}.[48,49] Both require transition and/or state dipole moments along two axes, and therefore a two-dimensional molecular structure. Thus, we select X-shaped, Λ-shaped, and octupolar molecules as subjects of investigation, based on several literature reports of large off-diagonal hyperpolarizabilities.[50−57] Figure 3 shows examples of high performance and archetypal 2-D chromophores that exhibit the basic attributes required for large γ_{zzxx}. In this section, we identify some intriguing design guidelines for γ_{zzxx} based on the structure types in Figure 3 by applying a three-state SOS/VB-CT model.

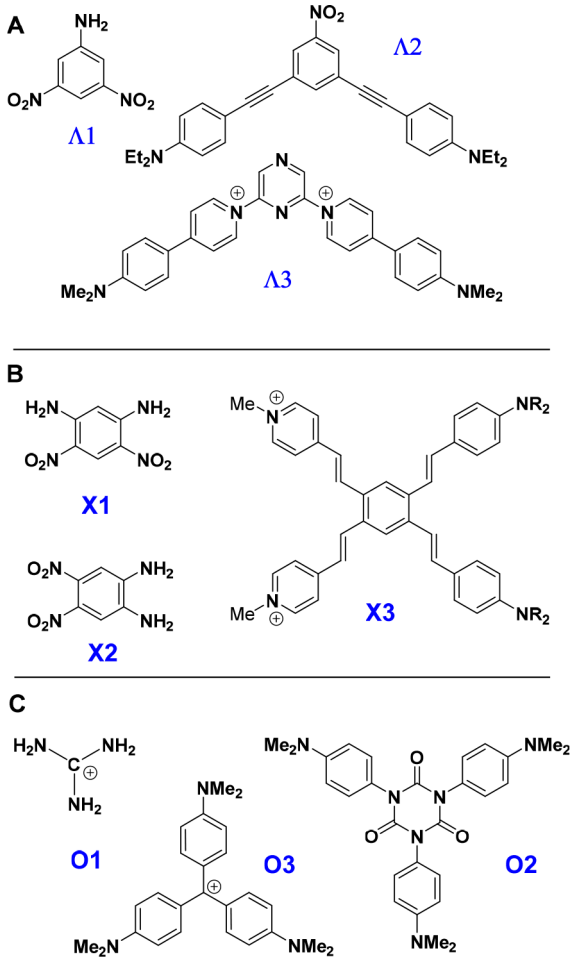

Figure 3. Examples of chromophores exhibiting large off-diagonal hyperpolarizability. **Λ1**, **X1**, **X2**, **O1**, **O2** are archetypal chromophores; the remaining structures represent more elaborate extensions. Counterions are omitted for clarity. Key: (A) Λ-shaped;[52,53] (B) X-shaped;[54] (C) octupolar.[50,51]

4.1. Three-State SOS Expression and VB-CT Approach.

To identify specific molecular attributes leading to enhanced γ_{zzxx}, we compute γ_{zzxx} for Λ-shaped, octupolar, and X-shaped VB-CT models using a three-state SOS expression. The VB and CT resonances of these systems are shown in Figure 4. Using

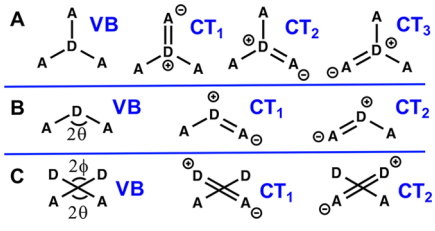

Figure 4. VB and CT contributions to γ_{zzxx} in the (A) octupolar, (B) Λ-shaped, and (C) X-shaped structures used for this analysis.

DOI: 10.1021/acs.jpcc.7b04307
J. Phys. Chem. C 2017, 121, 16491−16500

these resonances as a basis set we can construct a three-state Hamiltonian (see eq 15 below) for Λ-shaped and X-shaped molecules, from which we derive transition moments, excitation energies, and state dipole moments required to evaluate γ_{zzxx}. A similar four-state Hamiltonian yields the same information for octupolar molecules. We define E_{VB} and E_{CT} as the energies of the VB and CT configurations and $\Delta E = E_{VB} - E_{CT}$. $T = \langle CT_1|H|CT_2\rangle$, and $t = \langle VB|H|CT_1\rangle = \langle VB|H|CT_2\rangle$ are the transfer integrals, which represent the mixing of CT_1/CT_2 and CT/VB states, respectively.

$$H = \begin{pmatrix} E_{VB} & -t & -t \\ -t & E_{CT} & -T \\ -t & -T & E_{CT} \end{pmatrix} \tag{15}$$

One key metric in this analysis is the charge transfer character of the ground state, denoted l, which quantifies the weight of the CT configuration in the ground state. In literature l is defined as in eq 16 below, where $n + 1$ is the order of the Hamiltonian matrix.[40]

$$l \equiv \frac{1}{2n} - \frac{\Delta E - (n-1)T}{2n\sqrt{(\Delta E - (n-1)T)^2 + 4nt^2}} \tag{16}$$

The relevant transition and state dipole moments for dipolar, quadrupolar, octupolar, and Λ-shaped VB-CT models are available in the literature.[40−43]

In general, three essential states are found to be sufficient in describing NLO response,[33,40,58] so in order to calculate γ_{zzxx}, we consider a three-state expression derived from the full SOS theory.[46,59] This expression is

$$\begin{aligned}\gamma_{zzxx} = -4\Bigg[&\frac{(\mu_{01}^{z})^2(\mu_{01}^{x})^2}{E_{01}^{3}} + \frac{(\mu_{02}^{z})^2(\mu_{02}^{x})^2}{E_{02}^{3}} \\ &+ \frac{\mu_{01}^{x}\mu_{01}^{z}\mu_{02}^{x}\mu_{02}^{z}}{E_{01}^{2}E_{02}} + \frac{\mu_{01}^{x}\mu_{01}^{z}\mu_{02}^{x}\mu_{02}^{z}}{E_{01}E_{02}^{2}}\Bigg] \\ &+ 2\Bigg[\frac{\mu_{01}^{x}\mu_{01}^{z}\Delta\mu_{01}^{x}\Delta\mu_{01}^{z}}{E_{01}^{3}} + \frac{(\mu_{01}^{z})^2(\Delta\mu_{01}^{x})^2}{E_{01}^{3}} \\ &+ \frac{\mu_{02}^{x}\mu_{02}^{z}\Delta\mu_{02}^{x}\Delta\mu_{02}^{z}}{E_{02}^{3}} + \frac{(\mu_{02}^{z})^2(\Delta\mu_{02}^{x})^2}{E_{02}^{3}}\Bigg] \\ &+ 2\Bigg[\frac{\mu_{01}^{x}\mu_{01}^{z}\mu_{12}^{x}\mu_{12}^{z}}{E_{01}^{2}E_{02}} + \frac{(\mu_{01}^{z})^2(\mu_{12}^{x})^2}{E_{01}^{2}E_{02}} \\ &+ \frac{\mu_{02}^{x}\mu_{02}^{z}\mu_{12}^{x}\mu_{12}^{z}}{E_{01}E_{02}^{2}} + \frac{(\mu_{02}^{z})^2(\mu_{12}^{x})^2}{E_{01}E_{02}^{2}}\Bigg] \\ &+ 2\Bigg[\frac{\mu_{01}^{z}\Delta\mu_{01}^{x}\mu_{12}^{z}\mu_{02}^{x}}{E_{01}^{2}E_{02}} + 2\frac{\mu_{01}^{x}\Delta\mu_{01}^{z}\mu_{12}^{z}\mu_{02}^{x}}{E_{01}^{2}E_{02}} \\ &+ \frac{\mu_{01}^{x}\Delta\mu_{01}^{z}\mu_{12}^{x}\mu_{02}^{z}}{E_{01}^{2}E_{02}} + \frac{\mu_{02}^{z}\Delta\mu_{02}^{x}\mu_{12}^{z}\mu_{01}^{x}}{E_{01}E_{02}^{2}} \\ &+ 2\frac{\mu_{02}^{x}\Delta\mu_{02}^{z}\mu_{12}^{z}\mu_{01}^{x}}{E_{01}E_{02}^{2}} + \frac{\mu_{02}^{x}\Delta\mu_{02}^{z}\mu_{12}^{x}\mu_{01}^{z}}{E_{01}E_{02}^{2}}\Bigg]\end{aligned} \tag{17}$$

As with the three-state model for γ_{xxxx}, eq 17 can be organized into distinct and physically meaningful terms (shown in brackets) the first three of which are denoted as negative, dipolar, and two-photon, respectively. Although the detuning denominators in the resonant SOS expression[33] for γ suggest that M-E susceptibility is frequency-dependent and potentially resonantly enhanced, we limit our discussion to the static case.

4.2. Λ-Shaped Molecules (Figure 3A). Substitution of the relevant transition moments,[43] state dipole moments, and energies into eq 17 yields an expression for γ_{zzxx} for any Λ-shaped molecule, as given by eq 18. Valence band and charge transfer state configurations are illustrated for such molecules in Figure 4B.

$$\gamma_{zzxx} = \mu^4 \sin^2(\theta)\cos^2(\theta)\left[\frac{2l(1-2l)^2}{(2T + t\sqrt{1/l - 2})^3} + \frac{2l^{3/2}(1-2l)^{5/2}}{t(2T + t\sqrt{1/l - 2})^2}\right] \tag{18}$$

In Figure 5 the values of γ_{zzxx} calculated from eq 18 are plotted versus the CT character of the ground state, in the range $0 < l <$

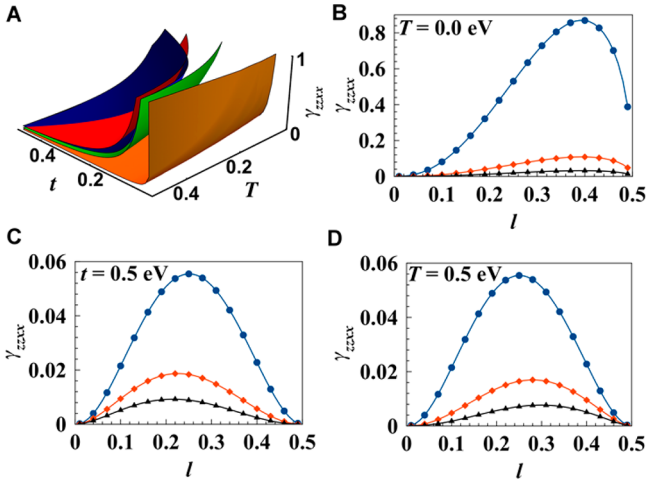

Figure 5. Λ-shaped and X-shaped chromophore γ_{zzxx} dependence on parameters l (charge transfer character), t, T. All values of l, t, T are expressed in eV, and γ_{zxzx} is in arbitrary units. (A) Dependence of γ_{zxzx} on t and T for $l = 0.01$ (orange), 0.1 (green), 0.2 (red), 0.3 (blue). Plots of l vs γ_{zxzx} in arbitrary units: (B) $T = 0$, $t = 0.5$ (circles), 1.0 (diamonds), 1.5 (triangles); (C) $t = 0.5$, $T = 0.5$, 1.0, 1.5; (D) $T = 0.5$, $t = 0.5$, 1.0, 1.5.

0.5. Other quantities appearing in eq 18 include the half angle θ between the two CT axes (see Figure 4B) and the magnitude of the dipole moment μ for the CT configuration. Only two terms from eq 17 are nonzero, so that γ_{zzxx} depends solely on a dipolar and "triangular" contribution. Because there is no contribution from the two-photon and negative terms, the present design rules are more likely to follow those for dipolar chromophores such as **$PMe_3TC_6(CN)_2$** (Figure 2) rather than chromophores relying on large transition moments of low-lying excitations as in **Se-8** (Figure 2) which derive their nonlinearity primarily from the negative term.[27]

With eq 18 in hand, we can investigate the dependence of γ_{zzxx} on l, t, and T (Figure 5). Figure 5A reveals an inverse relationship between γ_{zzxx} and t for all values of l. Broadly speaking, t refers the ability of the bridge connecting donor and acceptor fragments to efficiently mix the parent orbitals. In a physical sense, small values of t indicate a "purer" VB or CT character of the ground state, meaning that the resulting HOMO closely resembles one of the

DOI: 10.1021/acs.jpcc.7b04307
J. Phys. Chem. C 2017, 121, 16491−16500

parent orbitals. As such, bridging motifs which result in poor electronic connectivity between donor and acceptor are likely to effectively lower *t*. Some of these are illustrated in Figure 6.

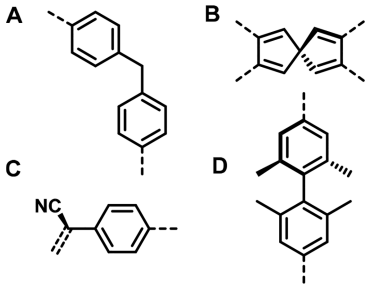

Figure 6. Bridging motifs exhibiting poor or disrupted conjugation: (A) spatial separation; (B) torsion enforced by structural connectivity; (C, D) torsion enforced by steric repulsion.

Twisted π-systems (TICT; Figure 2) are well-known to yield small *t* values, and to produce HOMOs that closely resemble the parent donor orbitals.[60−62] In TICT molecules, the inefficient electronic connectivity is evidenced by a weak charge transfer excitation relative to analogous planar molecules, and as the torsional angle is increased, the HOMO and LUMO become increasingly localized, consistent with decreased *t*.[63,64] Very large second- and third-order NLO response has been predicted and realized in donor−π−acceptor (D−π−A) chromophores with disrupted conjugation, including TICT chromophores and spiro-conjugated molecules.[30,65−68] Such observations are further supported by quantum graph studies of Kuzyk and Lytel, where they demonstrate that phase disruption can enhance NLO response.[34,69] Therefore, we recognize that the observed relationship in Figure 5A is consistent with previous experimental and theoretical work, and that *t* is a critical factor in enhancing γ.

At large values of *l*, γ_{zzxx} also exhibits an inverse dependence on *T*. While the same strategies can be employed to reduce *T*, the use of isolated D−π−A pairs can achieve the same effect. In structures such as **Λ1** (Figure 3A) the shared donor moiety mediates CT_1/CT_2 mixing, likely resulting in a large value of *T*. However, structures which contain two D−π−A pairs, such as molecule **Λ2** (Figure 3A), may reasonably be approximated by $T = 0$ due to the lack of electronic connectivity.

The general dependence of γ_{zzxx} on *l* varies over a range of *T* and *t* values (Figure 5B−D). When $t = 0.5$ eV (Figure 5C), increasing *T* leads to a slight decrease in the optimal CT character; when $T = 0.5$ eV (Figure 5B), increasing *t* causes a slight increase in optimal CT character; when $T = 0$ (Figure 5B), very large CT character results in the largest γ_{zzxx} regardless of the *t* value. *For the cases shown in* Figures 5D and 5C, *an intermediate CT contribution is required for enhancing* γ_{zzxx}, *and in the case of* Figure 5B, *structures with predominantly CT character will have the highest* γ_{zzxx} *for any value of t*. The need for intermediate *l* suggests that a trade-off between *l* and *t* is critical to obtaining the optimum performance since simply minimizing *t* would result in a purely CT or VB ground state, with $l = 0$ or $l = 0.5$. With exception of case 5B, careful manipulation of the bridging moiety is required to achieve the optimum performance. However, if the D−π−A pairs can be separated, then simply minimizing *t* could prove to be a rewarding approach. Because a large degree of CT character is desired in this case, *it is imperative that the CT state be lower in energy than the VB state* so that it may contribute strongly to the ground state character. This point is discussed in more detail in Section 4.4.

The design rules pertaining to the positioning of donor and acceptor moieties are much more straightforward. By inspection of eq 18, note that γ_{zzxx} increases as θ approaches 45°, although from a practical standpoint, upward of 75% of the maximum performance can be achieved within ±15°. Therefore, systems with sp^2 hybridized carbon and *meta*-substituted six-membered aromatics (both $\theta = 60°$), *ortho*-substituted five-membered heterocycles ($\theta = 36°$), and *ortho*-substituted six-membered aromatics ($\theta = 30°$) have the appropriate geometry for a large response.

4.3. X-Shaped Molecules (Figure 3B). If the charge transfer *between* adjacent D−π−A pairs can be neglected compared to the charge transfer *within* a pair, the effective Hamiltonians for X-shaped and Λ-shaped chromophores (Figure 3A, B) are identical, giving rise to the same eigenvalues and eigenfunctions. This is reasonable in the case of *meta* versus *para* CT in arenes[55] (see structure **X2**), although it may not hold for cases such as structure **X1** (Figure 3B), which likely requires a five-state analysis. Making the usual assumption that $\langle VB|\hat{\mu}|CT_1\rangle = \langle VB|\hat{\mu}|CT_2\rangle = \langle CT_1|\hat{\mu}|CT_2\rangle = 0$, we derive state and transition dipole moment eqs S27−S32, and substitute them into eq 15 to obtain eq 19.

$$\gamma_{zzxx} = \mu^4(\sin\theta + \sin\phi)^2(\cos\theta + \cos\phi)^2 \times \left[\frac{2l(1-2l)^2}{(2T + t\sqrt{1/l - 2})^3} + \frac{2l^{3/2}(1-2l)^{5/2}}{t(2T + t\sqrt{1/l - 2})^2}\right] \quad (19)$$

In eq 19, θ is the half angle between the two acceptor groups, and ϕ the half angle between the two donor substituents. Again, the optimal angle is $\theta = \phi = 45°$. Ultimately, the analysis at this level leads to the same results for *X*- and Λ-shaped chromophores in terms of dependence on *l*, *T*, *t*, and θ (Figure 5). One particular difference is the separation of the two CT states; here the assumption that *T* is very small is implicit in our model, since the two D−π−A pairs are taken as noninteracting. In this sense, we would expect an X-shaped chromophore to be described best by Figure 5B, and to have the highest performance when *l* approaches $^1/_2$, and *t* is very small.

On the basis of the μ^4 term in eq 18, X-shaped chromophores offer higher potential γ_{zzxx} than Λ-shaped analogues due to the enhanced CT dipole moments arising from additional donor or acceptor groups. Furthermore, there is reason to expect that X-shaped chromophores will provide large γ_{zzxx} values judging from literature reports on two-dimensional tetraethynylenthenes (TEE). Such molecules demonstrate large γ, and although the contribution of specific tensor elements has not yet reported, the two-dimensional arrangement of donor and acceptor moieties is well-situated for off-diagonal response.[70−72]

4.4. Octupolar Molecules (Figure 3C). The relevant transition moments and energies for octupolar molecules were derived by Cho et al.,[41,42] and utilized for a brief investigation of γ_{zzxx}.[41] Here, we investigate this model more explicitly, particularly in terms of *t* and *l* in order to create more general guidelines. Because the relevant transition and state dipole moments all have *x* and *z* components, all terms in eq 17 contribute to γ_{zzxx} for octupolar molecules. The expression reduces to

DOI: 10.1021/acs.jpcc.7b04307
J. Phys. Chem. C 2017, 121, 16491−16500

$$\gamma_{zzxx} = \frac{3\mu^4\left(l - \frac{9}{4}l^2\right)}{8(3T + t(\sqrt{1/l - 3}))^3} \quad (20)$$

In eq 20 the magnitudes of t and T have little impact on the overall behavior of γ_{zzxx} with respect to l. *Across a broad range of t and T, the maximum value of* γ_{zzxx} *occurs at* $l = {}^1/_3$. The design parameters are then straightforward; increasing CT character while lowering t and T is clearly the key to higher performance (Figure 7). Thus, it may be useful to employ a segmented or

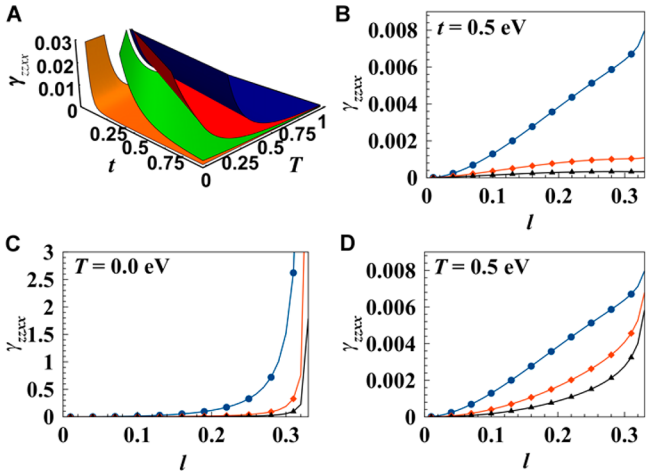

Figure 7. Octupolar chromophore γ_{zzxx}dependence on l, t, T. All values of l, t, T are expressed in eV and γ_{zzxx} is in arbitrary units. (A) Dependence of γ_{zzxx} on t and T for l = 0.01 (orange), 0.1 (green), 0.2 (red), and 0.3 (blue). Plots of l vs γ_{zzxx} in arbitrary units: (B) T = 0, t = 0.5 (circles), 1.0 (diamonds), 1.5 (triangles); (C) t = 0.5, T = 0.5, 1.0, 1.5; (D) T = 0.5, t = 0.5, 1.0, 1.5.

multiple donor/acceptor paradigm to reduce T; for example, moving from **O3** to **O2** (Figure 3C) allows a degree of isolation between CT states. Similar to the Λ-shaped and X-shaped cases, γ_{zzxx} exhibits an inverse dependence on t (Figure 7A). Therefore, the same disrupted conjugation pathways suggested in Section 4.2 should apply to octupolar structures as well. However, in this case there is no trade-off between l and t, so t can simply be minimized. Finally, the strong CT character of the ground state, in the absence of significant VB/CT mixing, requires that the CT resonance be lower in energy than the VB resonance. Such structures with high CT character are known in the literature and can be readily identified by their strong, negative solvatochromism.[73] In these cases, the CT state may be stabilized by aromaticity, inductive effects, charge delocalization, or interactions with the chromophore environment.[74−78] Another approach is to destabilize the VB resonance by introducing geometric constraints.[65,66,79]

4.5. VB-CT Conclusions. SOS based analysis of the VB-CT models discussed here provides intriguing molecular structure-based design criteria for optimizing molecular M-E polarization. Specifically,

(i) For each structure type, γ_{zzxx} is proportional to μ^4, so inclusion of strong donor and acceptor moieties, and extension of the CT spatial length will be beneficial insofar as it does not negatively impact VB/CT mixing.[46,80−83]

(ii) A brief inspection of θ and ϕ reveals the optimal geometry for off-diagonal response is accessible through common organic molecular structural geometries.

(iii) The complex dependency of γ_{zzxx} on l suggests that for Λ- and X-shaped chromophores, moderate to large l leads to large, positive γ_{zzxx}. For octupolar molecules, l must simply be maximized. In both cases, it is clear that enhanced CT character in the ground state must be targeted (discussed in Sections 4.2 and 4.4) by lowering the CT state energy or raising the energy of the VB state.

(iv) The inverse dependence on T and t suggests that bridging motifs (Figure 6) which disrupt conjugation will lead to enhanced NLO performance, though care must be taken to maintain the optimal CT character.

In general, many of the same conceptual avenues used for conventional NLO chromophores should be productively applicable to new chromophore geometries designed to achieve enhanced M-E rectification.

5. SUMMARY

Magneto-electric magnetization and rectification processes at the molecular level are relatively new nonlinear effects for which the design principles are absent in the scientific literature. Here we have demonstrated a relationship between the all-electric susceptibility elements $\chi^{(3)}_{xxxx}$ and $\chi^{(3)}_{zzxx}$, and the two lowest-order magneto-electric processes, magnetization and rectification respectively, and have exploited it to outline strategies for enhancing these effects. For example, cyanines and typical 1-D donor-π-acceptor chromophores are predicted to be good candidates for M-E magnetization, given their very large values of $\chi^{(3)}_{xxxx}$. In fact, many of the current high performance third-order NLO materials are likely to exhibit strong induced M-E magnetization.

In the case of M-E rectification, the guidelines for optimal material synthesis are less specific. There has been little investigation to date of anisotropic hyperpolarizability elements such as γ_{zzxx}, so it is difficult to identify chromophores suitable for M-E rectification. Our analysis of γ_{zzxx} in VB-CT models has nevertheless identified rational design criteria for three common structure types, which are by no means exhaustive. From this result, it is clear that a significant CT contribution to the ground state is necessary, as are large static dipole moments. Extending conjugation, increasing D/A strength, and disrupting conjugation are all promising tools for tuning the CT contribution in the context of Λ-shaped, X-shaped, and octupolar molecules. On the other hand, these design rules are far from complete. Excited state charge transfer dynamics have not been addressed in this analysis, although they are likely to be an important component of M-E response. From an experimental standpoint, the finding that large static dipole moments may increase the value of $\chi^{(3)}_{zzxx}$ could prove to be problematic for the interpretation of scattering experiments, as internal moments facilitate molecular alignment by applied electric fields thereby altering the depolarization ratio which may otherwise be determined by magneto-electric processes. Nevertheless, the present work should serve as the first step toward the rational design of M-E materials exhibiting enhanced nonlinearity that can be tailored to meet specific magneto-electric applications.

■ ASSOCIATED CONTENT

Supporting Information

The Supporting Information is available free of charge on the ACS Publications website at DOI: 10.1021/acs.jpcc.7b04307.

DOI: 10.1021/acs.jpcc.7b04307
J. Phys. Chem. C 2017, 121, 16491−16500

Details of the derivations summarized in section 2 and transition and dipole moments of X-shaped molecules (PDF)

AUTHOR INFORMATION

Corresponding Authors

*(T.J.M.) E-mail: t-marks@northwestern.edu.
*(S.C.R.) E-mail: scr@umich.edu.

ORCID

Tobin J. Marks: 0000-0001-8771-0141

Author Contributions

‡These authors contributed equally.

Notes

The authors declare no competing financial interest.

ACKNOWLEDGMENTS

This work was supported by AFOSR MURI Grant FA9550_14_1_0040. A.J.-T.L thanks the NDSEG and E.F.C.D. thanks the NSF for graduate research fellowships. The authors also wish to acknowledge useful discussions with D. Hagan and E. Van Stryland.

REFERENCES

(1) Shi, Y.; Zhang, C.; Zhang, H.; Bechtel, J.; Dalton, L.; Robinson, B. H.; Steier, W. Low (Sub-1-V) Halfwave Voltage Polymeric Electro-optic Modulators Achieved by Controlling Chromophore Shape. *Science* **2000**, *288*, 119−122.

(2) Lee, M.; Katz, H.; Erben, C.; Gill, D.; Gopalan, P.; Heber, J.; McGee, D. Broadband Modulation of Light by Using an Electro-Optic Polymer. *Science* **2002**, *298*, 1401−1403.

(3) Koos, C.; Vorreau, P.; Vallaitis, T.; Dumon, P.; Bogaerts, W.; Baets, R.; Esembeson, B.; Biaggio, I.; Michinobu, T.; Diederich, F.; et al. All-Optical High-speed Signal Processing with Silicon−Organic Hybrid Slot Waveguides. *Nat. Photonics* **2009**, *3*, 216−219.

(4) Raymo, F. M.; Giordani, S. All-optical Processing with Molecular Switches. *Proc. Natl. Acad. Sci. U. S. A.* **2002**, *99*, 4941−4944.

(5) Dalton, L. R. Nonlinear Optical Polymeric Materials: From Chromophore Design to Commercial Applications. *Adv. Polym. Sci.* **2002**, *158*, 1−76.

(6) Kajzar, F.; Lee, K.-S.; Jen, A. K. Polymeric Materials and their Orientation Technique for Second-Order Nonlinear Optics. *Adv. Polym. Sci.* **2003**, *161*, 1−80.

(7) Shen, Y. R. Surface Properties Probed by Second-Harmonic and Sum-Frequency Generation. *Nature* **1989**, *337*, 519−525.

(8) Dini, D.; Calvete, M. J.; Hanack, M. Nonlinear Optical Materials for the Smart Filtering of Optical Radiation. *Chem. Rev.* **2016**, *116*, 13043−13233.

(9) Chai, Z.; Hu, X.; Wang, F.; Niu, X.; Xie, J.; Gong, Q. Ultrafast All-Optical Switching. *Adv. Opt. Mater.* **2017**, *5*, 1600665.

(10) Grigorenko, A. N.; Geim, A. K.; Gleeson, H. F.; Zhang, Y.; Firsov, A. A.; Khrushchev, I. Y.; Petrovic, J. Nanofabricated Media with Negative Permeability at Visible Frequencies. *Nature* **2005**, *438*, 335−338.

(11) Hoffman, A. J.; Alekseyev, L.; Howard, S. S.; Franz, K. J.; Wasserman, D.; Podolskiy, V. A.; Narimanov, E. E.; Sivco, D. L.; Gmachl, C. Negative Refraction in Semiconductor Metamaterials. *Nat. Mater.* **2007**, *6*, 946−950.

(12) Smith, D. R.; Pendry, J. B.; Wiltshire, M. C. K. Metamaterials and Negative Refractive Index. *Science* **2004**, *305*, 788−792.

(13) Schurig, D.; Mock, J. J.; Justice, B. J.; Cummer, S. A.; Pendry, J. B.; Starr, A. F.; Smith, D. R. Metamaterial Electromagnetic Cloak at Microwave Frequencies. *Science* **2006**, *314*, 977−979.

(14) Shalaev, V. M. Optical Negative-Index Metamaterials. *Nat. Photonics* **2007**, *1*, 41−48.

(15) Pendry, J. B. Negative Refraction Makes a Perfect Lense. *Phys. Rev. Lett.* **2000**, *85*, 3966−3969.

(16) Shelby, R. A.; Smith, D. R.; Schultz, S. Experimental Verification of a Negative Index of Refraction. *Science* **2001**, *292*, 77−79.

(17) Monticone, F.; Alù, A. The Quest for Optical Magnetism: From Split-Ring Resonators to Plasmonic Nanoparticles and Nanoclusters. *J. Mater. Chem. C* **2014**, *2*, 9059−9072.

(18) Oliveira, S. L.; Rand, S. C. Intense Nonlinear Magnetic Dipole Radiation at Optical Frequencies: Molecular Scattering in a Dielectic Liquid. *Phys. Rev. Lett.* **2007**, *98*, 093901.

(19) Rand, S. C.; Fisher, W. M.; Oliveira, S. L. Optically-Induced Magnetism in Dielectric Media. *J. Opt. Soc. Am. B* **2008**, *25*, 1106−1117.

(20) Fisher, W. M.; Rand, S. C. Optically-Induced Charge Separation and Terahertz Emission in Unbiased Dielectrics. *J. Appl. Phys.* **2011**, *109*, 064903.

(21) Rand, S. C. Quantum Theory of Coherent Transverse Optical Magnetism. *J. Opt. Soc. Am. B* **2009**, *26*, B120−B129.

(22) Fisher, A. A.; Cloos, E. F.; Fisher, W. M.; Rand, S. C. Dynamic Symmetry-Breaking in a Simple Quantum Model of Magneto-Electric Rectification, Optical Magnetization, and Harmonic Generation. *Opt. Express* **2014**, *22*, 2910−2924.

(23) Fisher, A. A.; Dreyer, E. F. C.; Chakrabarty, A.; Rand, S. C. Optical Magnetization, Part II: Theory of Induced Optical Magnetism. *Opt. Express* **2016**, *24*, 26055.

(24) Fisher, A. A.; Dreyer, E. F. C.; Chakrabarty, A.; Rand, S. C. Optical Magnetization, Part I: Experiments on Radiant Optical Magnetization in Solids. *Opt. Express* **2016**, *24*, 26064.

(25) Marder, S. R. Organic Nonlinear Optical Materials: Where We Have Been and Where We are Going. *Chem. Commun.* **2006**, 131−134.

(26) Prasad, P. N.; Williams, D. J. *Introduction to Nonlinear Optical Effects in Molecules and Polymers*; John Wiley & Sons: New York, 1991.

(27) Hales, J. M.; Barlow, S.; Kim, H.; Mukhopadhyay, S.; Brédas, J.-L.; Perry, J. W.; Marder, S. R. Design of Organic Chromophores for All-Optical Signal Processing Applications. *Chem. Mater.* **2014**, *26*, 549−560.

(28) Hales, J. M.; Matichak, J. D.; Barlow, S.; Ohira, S.; Yesudas, K.; Bredas, J. L.; Perry, J. W.; Marder, S. R. Design of Polymethine Dyes with Large Third-Order Optical Nonlinearities and Loss Figures of Merit. *Science* **2010**, *327*, 1485−1487.

(29) Teran, N. B.; He, G. S.; Baev, A.; Shi, Y.; Swihart, M. T.; Prasad, P. N.; Marks, T. J.; Reynolds, J. R. Twisted Thiophene-Based Chromophores with Enhanced Intramolecular Charge Transfer for Cooperative Amplification of Third-Order Optical Nonlinearity. *J. Am. Chem. Soc.* **2016**, *138*, 6975−6984.

(30) He, G. S.; Zhu, J.; Baev, A.; Samoc, M.; Frattarelli, D. L.; Watanabe, N.; Facchetti, A.; Agren, H.; Marks, T. J.; Prasad, P. N. Twisted Pi-System Chromophores: Novel Pathway to All-Optical Switching. *J. Am. Chem. Soc.* **2011**, *133*, 6675−6680.

(31) Bredas, J. L.; Adant, C.; Tackx, P.; Persoons, A.; Pierce, B. M. Third-Order Nonlinear Optical Response in Organic Materials: Theoretical and Experimental Aspects. *Chem. Rev.* **1994**, *94*, 243−278.

(32) Gieseking, R. L.; Mukhopadhyay, S.; Risko, C.; Marder, S. R.; Bredas, J. L. 25th Anniversary Article: Design of Polymethine Dyes for All-Optical Switching Applications: Guidance from Theoretical and Computational Studies. *Adv. Mater.* **2014**, *26*, 68−83.

(33) Ensley, T. R.; Hu, H.; Reichert, M.; Ferdinandus, M. R.; Peceli, D.; Hales, J. M.; Perry, J. W.; Li, Z. A.; Jang, S.-H.; Jen, A. K. Y.; et al. Quasi-Three-Level Model Applied to Measured Spectra of Nonlinear Absorption and Refraction in Organic Molecules. *J. Opt. Soc. Am. B* **2016**, *33*, 780−796.

(34) Lytel, R.; Mossman, S. M.; Kuzyk, M. G. Phase Disruption as a New Design Paradigm for Optimizing the Nonlinear-Optical Response. *Opt. Lett.* **2015**, *40*, 4735−4738.

(35) Shi, Y.; Lou, A. J.-T.; He, G. S.; Baev, A.; Swihart, M. T.; Prasad, P. N.; Marks, T. J. Cooperative Coupling of Cyanine and Tictoid Twisted Pi-Systems to Amplify Organic Chromophore Cubic Nonlinearities. *J. Am. Chem. Soc.* **2015**, *137*, 4622−4625.

(36) Li, Z. a.; Ensley, T. R.; Hu, H.; Zhang, Y.; Jang, S.-H.; Marder, S. R.; Hagan, D. J.; Van Stryland, E. W.; Jen, A. K. Y. Conjugated

DOI: 10.1021/acs.jpcc.7b04307
J. Phys. Chem. C 2017, 121, 16491−16500

Polycyanines: A New Class of Materials with Large Third-Order Optical Nonlinearities. *Adv. Opt. Mater.* **2015**, *3*, 900−906.
(37) Michinobu, T.; May, J. C.; Lim, J. H.; Boudon, C.; Gisselbrecht, J. P.; Seiler, P.; Gross, M.; Biaggio, I.; Diederich, F. A New Class of Organic Donor-Acceptor Molecules with Large Third-Order Optical Nonlinearities. *Chem. Commun.* **2005**, 737−739.
(38) Terenziani, F.; Przhonska, O. V.; Webster, S.; Padilha, L.; Slominsky, Y.; Davydenko, I.; Gerasov, A.; Kovtun, Y.; Shandura, M.; Kachkovski, A.; et al. Essential-State Model for Polymethine Dyes: Symmetry Breaking and Optical Spectra. *J. Phys. Chem. Lett.* **2010**, *1*, 1800−1804.
(39) Boldrini, B.; Cavalli, E.; Painelli, A.; Terenziani, F. Polar Dyes in Solution: A Joint Experimental and Theoretical Study of Absorption and Emission Band Shapes. *J. Phys. Chem. A* **2002**, *106*, 6286−6294.
(40) Cho, M.; An, S.-Y.; Lee, H.; Ledoux, I.; Zyss, J. Nonlinear Optical Properties of Tetrahedral Donor−Acceptor Octupolar Molecules: Effective Five-State Model Approach. *J. Chem. Phys.* **2002**, *116*, 9165−9173.
(41) Cho, M.; Kim, H.-S.; Jeon, S.-J. An Elementary Description of Nonlinear Optical Properties of Octupolar Molecules: Four-State Model for Guanidinium-Type Molecules. *J. Chem. Phys.* **1998**, *108*, 7114−7120.
(42) Lee, Y.-K.; Jeon, S.-J.; Cho, M. Molecular Polarizability and First Hyperpoalrizabtility of Octupolar Molecules: Donor-Substituted Triphenylmethane Dyes. *J. Am. Chem. Soc.* **1998**, *120*, 10921−10927.
(43) Yang, M.; Champagne, B. Large Off-Diagonal Contribution to the Second-Order Nonlinearities of L-Shaped Molecules. *J. Phys. Chem. A* **2003**, *107*, 3942−3951.
(44) Balanis, C. A. *Advanced Engineering Electromagnetics*; John Wiley & Sons, Inc.: New York, 1989.
(45) Fisher, A. A.; Cloos, E. F.; Fisher, W. M.; Rand, S. C. Dynamic Symmetry-Breaking in a Simple Quantum Model of Magneto-Electric Rectification, Optical Magnetization, and Harmonic Generation. *Opt. Express* **2014**, *22*, 2910.
(46) Gubler, U.; Bosshard, C. Molecular Design for Third-Order Nonlinear Optics. *Adv. Polym. Sci.* **2002**, *158*, 123−187.
(47) Kuzyk, M. G.; Singer, K. D.; Stegeman, G. I. Theory of Molecular Nonlinear Optics. *Adv. Opt. Photonics* **2013**, *5*, 4.
(48) Gorman, C.; Marder, S. R. Effect of Molecular Polarization on Bond-Length Alternation, Linear Polarizability, First and Second Hyperpolarizability in Donor-Acceptor Polyenes as a Function of Chain Length. *Chem. Mater.* **1995**, *7*, 215−220.
(49) Meyers, F.; Marder, S. R.; Pierce, B. M.; Bredas, J. L. Electric Field Modulated Nonlinear Optical Properties of Donor Acceptor Polyenes: Sum-Over-States Investigation of the Relationship Between Molecular Polarizabiltiesi (α, β, and γ) and Bond Length Alternation. *J. Am. Chem. Soc.* **1994**, *116*, 10703−10714.
(50) Argouarch, G.; Veillard, R.; Roisnel, T.; Amar, A.; Boucekkine, A.; Singh, A.; Ledoux, I.; Paul, F. Donor-Substituted Triaryl-1,3,5-triazinanes-2,4,6-triones: Octupolar NLO-phores with a Remarkable Transparency−Nonlinearity Trade-off. *New J. Chem.* **2011**, *35*, 2409.
(51) Verbiest, T.; Clays, K.; Samyn, C.; Wolff, J.; Reinhoudt, D.; Persoons, A. Investigation of the Hyperpolarizability in Organic Molecules from Dipolar to Octopolar Systems. *J. Am. Chem. Soc.* **1994**, *116*, 9320−9323.
(52) Coe, B. J.; Fielden, J.; Foxon, S. P.; Helliwell, M.; Asselberghs, I.; Clays, K.; De Mey, K.; Brunschwig, B. S. Syntheses and Properties of Two-Dimensional, Dicationic Nonlinear Optical Chromophores Based on Pyrazinyl Cores. *J. Org. Chem.* **2010**, *75*, 8550−8563.
(53) Ramirez, M. A.; Cuadro, A. M.; Alvarez-Builla, J.; Castano, O.; Andres, J. L.; Mendicuti, F.; Clays, K.; Asselberghs, I.; Vaquero, J. J. Donor-(pi-Bridge)-azinium as D-pi-A+ One-Dimensional and D-pi-A(+)-pi-D Multidimensional V-Shaped Chromophores. *Org. Biomol. Chem.* **2012**, *10*, 1659−1669.
(54) Kang, H.; Evmenenko, G.; Dutta, P.; Clays, K.; Song, K.; Marks, T. J. X-Shaped Electro-optic Chromophore with Remarkably Blue-Shifted Optical Absorption. Synthesis, Characterization, Linear/Nonlinear Optical Properties, Self-Assembly, and Thin Film Microstructural Characteristics. *J. Am. Chem. Soc.* **2006**, *128*, 6194−6205.
(55) Oliva, M. M.; Casado, J.; Hennrich, G.; López Navarrete, J. T. Octopolar Chromophores Based on Donor- and Acceptor-Substituted 1,3,5-Tris(phenylethynyl)benzenes: Impact of Meta-Conjugation on the Molecular and Electronic Structure by Means of Spectroscopy and Theory. *J. Phys. Chem. B* **2006**, *110*, 19198−19206.
(56) Traber, B.; Oeser, T.; Gleiter, R.; Goebel, M.; Wortmann, R. D. Donor-Substituted Heptaazaphenalene as a Nonlinear Optically Active Molecule with Multiple Charge-Transfer Transitions. *Eur. J. Org. Chem.* **2004**, *2004*, 4387−4390.
(57) Wortmann, R.; Lebus-Henn, S.; Reis, H.; Papadopoulos, M. G. Off-Diagonal Second-Order Polarizability of N,N′-dihexyl-1,3-diamino-4,6-dinitrobenzene. *J. Mol. Struct.: THEOCHEM* **2003**, *633*, 217−226.
(58) Dirk, C. W.; Cheng, L.-T.; Kuzyk, M. G. A Simplified Three-Level Model Describing the Molecular Third-Order Nonlinear Optical Susceptibility. *Int. J. Quantum Chem.* **1992**, *43*, 27−36.
(59) Orr, B. J.; Ward, J. F. Perturbation Theory of the Non-linear Optical Polarization of an Isolated System. *Mol. Phys.* **1971**, *20*, 513−526.
(60) Metzger, R. M. Unimolecular Electrical Rectifiers. *Chem. Rev.* **2003**, *103*, 3803−3834.
(61) Terenziani, F.; Painelli, A.; Girlando, A.; Metzger, R. M. From Solution to Langmuir-Blodgett Films: Spectroscopic Study of a Zwitterionic Dye. *J. Phys. Chem. B* **2004**, *108*, 10743−10750.
(62) Grisanti, L.; D'Avino, G.; Painelli, A.; Guasch, J.; Ratera, I.; Veciana, J. Essential State Models for Solvatochromism in Donor-Acceeptor Molecules: The Role of the Bridge. *J. Phys. Chem. B* **2009**, *113*, 4718−4725.
(63) Shi, Y.; Frattarelli, D.; Watanabe, N.; Facchetti, A.; Cariati, E.; Righetto, S.; Tordin, E.; Zuccaccia, C.; Macchioni, A.; Wegener, S. L.; et al. Ultra-High-Response, Multiply Twisted Electro-optic Chromophores: Influence of pi-System Elongation and Interplanar Torsion on Hyperpolarizability. *J. Am. Chem. Soc.* **2015**, *137*, 12521−12538.
(64) Wang, Y.; Frattarelli, D. L.; Facchetti, A.; Cariati, E.; Tordin, E.; Ugo, R.; Zuccaccia, C.; Macchioni, A.; Wegener, S. L.; Stern, C. L.; et al. Twisted π-Electron System Electrooptic Chromophores. Structural and Electronic Consequences of Relaxing Twist-Inducing Nonbonded Repulsions. *J. Phys. Chem. C* **2008**, *112*, 8005−8015.
(65) Albert, I. D. L.; Marks, T. J.; Ratner, M. A. Conformationally-Induced Geometric Electron Localization. Interrupted Conjugation, Very Large Hyperpolarizabilities, and Sizale Infrared Absorption in Simple Twisted Molecular Chromophores. *J. Am. Chem. Soc.* **1997**, *119*, 3155−3156.
(66) Brown, E. C.; Ratner, M. A.; Marks, T. J. Nonlinear Response Properties of Ultralarge Hyperpolarizability Twisted Pi-System Donor-Accpetor Chromophores. *J. Phys. Chem. B* **2008**, *112*, 44−50.
(67) Kato, S.-i.; Beels, M. T. R.; La Porta, P.; Schweizer, W. B.; Boudon, C.; Gisselbrecht, J.-P.; Biaggio, I.; Diederich, F. Homoconjugated Push-Pull and Spiro Systems: Intramolecular Charge-Transfer Interactions and Third-Order Optical Nonlinearities. *Angew. Chem., Int. Ed.* **2010**, *49*, 6207−6211.
(68) Kang, H.; Facchetti, A.; Jiang, H.; Cariati, E.; Righetto, S.; Ugo, R.; Zuccaccia, C.; Macchioni, A.; Stern, C. L.; Marks, T. J.; et al. Ultra-large Hyperpolarizability Twisted pi-electron System Electro-Optic Chromophores. *J. Am. Chem. Soc.* **2007**, *129*, 3267−3286.
(69) Perez-Moreno, J.; Zhao, Y.; Clays, K.; Kuzyk, M. G. Modulated Conjugation as a Means for Attaining a Record High Intrinsic Hyperpolarizability. *Opt. Lett.* **2007**, *32*, 59−61.
(70) Tykwinski, R. R.; Gubler, U.; Martin, R.; Diederich, F.; Bosshard, C.; Gunter, P. Structure-Property Relationships in Third-Order Nonlinear Optical Chromophores. *J. Phys. Chem. B* **1998**, *102*, 4451−4465.
(71) Gubler, U.; Spreiter, R.; Bosshard, C.; Günter, P.; Tykwinski, R. R.; Diederich, F. Two-Dimensionally Conjugated Molecules: The Importance of Low Molecular Symmetry for Large Third-Order Nonlinear Optical Effects. *Appl. Phys. Lett.* **1998**, *73*, 2396−2398.
(72) Bosshard, C.; Spreiter, R.; Gunter, P.; Trkwinski, R. R.; Schreiber, M.; Diederich, F. Structure-Property Relationships in Nonlinear Optical Tetraethynylethenes. *Adv. Mater.* **1996**, *8*, 231−234.

DOI: 10.1021/acs.jpcc.7b04307
J. Phys. Chem. C 2017, 121, 16491−16500

(73) Sasaki, S.; Drummen, G. P. C.; Konishi, G.-i. Recent Advanecs in Twisted Intramolecuar Charge Transfer (TICT) Fluorescence and Related Phenomena in Materials Chemisty. *J. Mater. Chem. C* **2016**, *4*, 2731−2743.
(74) Kim, J. J.; Funabiki, K.; Muramatsu, H.; Shibata, K.; Kim, S. H.; Shiozaki, H.; Hartmann, H.; Matsui, M. Negative Solvatochromism of Azo Dyes Derived from (Dialkylamino)thiazole Dimers. *Chem. Commun.* **2000**, 753−754.
(75) Ishchenko, A. A.; Kulinich, A. V.; Bondarev, S. L.; Knyukshto, V. N. Electronic Structure and Fluorescent Properties of Malononitrile-Based Merocyanines with Positive and Negative Solvatochromism. *Opt. Spectrosc.* **2008**, *104*, 57−68.
(76) Meng, S.; Caprasecca, S.; Guido, C. A.; Jurinovich, S.; Mennucci, B. Negative Solvatochromism of Push-Pull Biphenyl Compounds: a Theoretical Study. *Theor. Chem. Acc.* **2015**, *134*, 150.
(77) Kulinich, A. V.; Mikitenko, E. K.; Ishchenko, A. A. Scope of Negative Solvatochromism and Solvatofluorochromism of Merocyanines. *Phys. Chem. Chem. Phys.* **2016**, *18*, 3444−3453.
(78) Warde, U.; Sekar, N. NLOphoric Mono-Azo Dyes with Negative Solvatochromism and In-Built ESIPT Unit from Ethyl 1,3-dihydroxy-2-naphthoate: Estimation of Excited State Dipole Moment and pH Study. *Dyes Pigm.* **2017**, *137*, 384−394.
(79) Jacques, P.; Graff, B.; Diemer, V.; Ay, E.; Chaumeil, H.; Carre, C.; Malval, J.-P. Negative Solvatochromism of a Series of Pyridinium Phenolate Betaine Dyes with Increasing Steric Hindrance. *Chem. Phys. Lett.* **2012**, *531*, 242−246.
(80) Alain, V.; Redoglia, S.; Blanchard-Desce, M.; Lebus, S.; Lukaszuk, K.; Wortmann, R.; Gubler, U.; Bosshard, C.; Gunter, P. Elongated Push-Pull Diphenylpolyenes for Nonlinear Optics: Molecular Engineering of Quadratic and Cubic Optical Nonlinearities via Tuning of Intramolecular Charge Transfer. *Chem. Phys.* **1999**, *245*, 51−71.
(81) Schmidt, K.; Barlow, S.; Leclercq, A.; Zojer, E.; Jang, S.-H.; Marder, S. R.; Jen, A. K. Y.; Bredas, J.-L. Efficient Acceptor Groups for NLO Chromophores: Competing Inductive and Resonance Contributions in Heterocyclic Acceptors Derived from 2-dicyanomethylidene-3-cyano-4,5,5-trimethyl-2,5-dihydrofuran. *J. Mater. Chem.* **2007**, *17*, 2944−2949.
(82) Leclercq, A.; Zojer, E.; Jang, S. H.; Barlow, S.; Geskin, V.; Jen, A. K.; Marder, S. R.; Bredas, J. L. Quantum-Chemical Investigation of Second-order Nonlinear Optical Chromophores: Comparison of Strong Nitrile-Based Acceptor End Groups and Role of Auxiliary Donors and Acceptors. *J. Chem. Phys.* **2006**, *124*, 044510.
(83) Salman, S.; Brédas, J.-L.; Marder, S. R.; Coropceanu, V.; Barlow, S. Dipolar Ferrocene and Ruthenocene Second-Order Nonlinear Optical Chromophores: A Time-Dependent Density Functional Theory Investigation of Their Absorption Spectra. *Organometallics* **2013**, *32*, 6061−6068.

DOI: 10.1021/acs.jpcc.7b04307
J. Phys. Chem. C 2017, 121, 16491−16500